THE DEVELOPMENT OF AN AIR BRAYTON AND A STEAM RANKINE SOLAR RECEIVER

by

M. Greeven, Project Engineer,
AiResearch Manufacturing Company of California

ABSTRACT

This paper describes both an air Brayton and a steam Rankine solar receiver now under development for the Department of Energy under contract to the Jet Propulsion Laboratory. These cavity receivers accept concentrated insolation from a single-point focus, parabolic concentrator, and use this energy to heat the working fluid. Both receivers have been designed for a solar input of 85 kw. The air Brayton receiver heats the air to 816°C (1500°F). A metallic plate-fin heat transfer surface is used in this unit to effect the energy transfer. The steam Rankine receiver has been designed as a once-through boiler with reheat. The receiver heats the water to 704°C (1300°F) to produce steam at 17.22 MPa (2500 psi) in the boiler section. The reheat section operates at 1.2 MPa (75 psi), reheating the steam to 704°C (1300°F). The paper discusses the thermal and mechanical design features of the Brayton receiver and reviews the design of the Rankine receiver.

AIR BRAYTON SOLAR RECEIVER

Design Requirements

The solar input is 85 kw. This energy is used to heat the working gas (air) of the highly recuperated open-cycle gas turbine engine from 565° to 816°C (1049° to 1500°F). The flow rate is 0.28 kg/sec (0.57 lb/sec) at an inlet pressure of 0.25 MPa (36.75 psia). The pressure drop goal is 2 percent $\Delta P/P_{IN}$. The solar input is provided by an 11-m (36-ft)-dia parabolic dish concentrator that has an assumed slope error of 1.75 milliradian, as well as a zero tracking error. (Slope error is a measure of the surface inaccuracies of the actual concentrator compared to that of an ideal surface.) In addition to the performance requirements, the environmental conditions included a 48.3-km/hr (30-mph) steady-state wind with a 20-percent gust factor; temperature extremes of -18 to 52°C (0° to 125°F); humidity extremes of 0 to 100 percent; and blowing dust. Survival environmental conditions such as 161 km/hr (100-mph) winds, seismic loads up to 3 g, and snow and ice loads also were imposed.

Receiver Description

The major elements of the receiver are shown in Figure 1. The outer cylindrical case is approximately 0.76 m (30 in.) in diameter by 1.71 m (46 in.) long. Mounting brackets attached to the surface of the case mate to a mounting ring that is part of the concentrator structure. A second inner cylindrical assembly forms the receiver cavity. Approximately 0.11 m (4.5 in.) of insulation are placed between the outer case and inner cavity. The wall of the receiver cavity consists of a single-sandwich, plate-fin heat exchanger panel. Air from the recuperator is ducted to a toroidal manifold at the bottom of the panel, where it flows up the annular passage that defines the vertical walls of the cylindrical cavity. It is subsequently collected in another toroidal manifold at the top of the cavity assembly, where it is ducted to the turbine inlet.

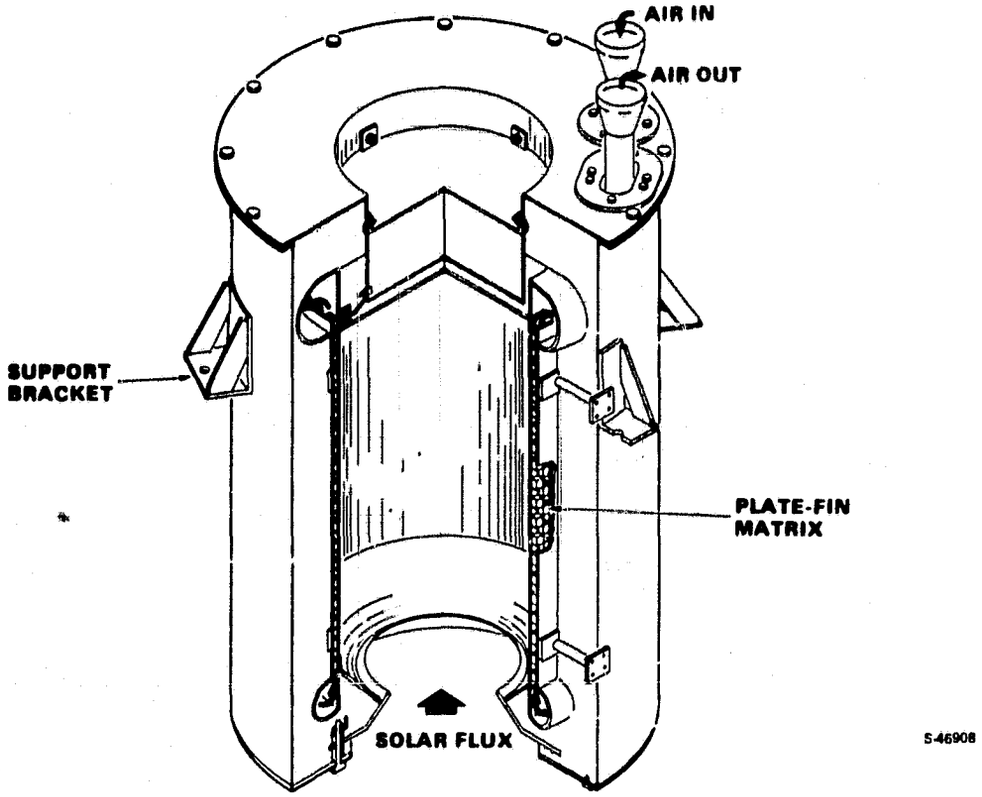

FIG. 1. PROTOTYPE AIR BRAYTON SOLAR RECEIVER

The single-sandwich cylindrical panel contains a high-density offset fin matrix. This matrix has 4.72 fins/cm (12 fins/in.), which are 1.27 cm (0.50 in.) high, 0.01 cm (0.004 in.) thick, with a 1.27 cm (0.50-in.) offset length. The fins are brazed to the two metal sheets that form the cylindrical panel. The heat exchanger is made from Inconel 625 material. The receiver is positioned so the focal point of the concentrator is located at the plane of the receiver aperture. The aperture end is a cone assembly made from silicon carbide, which forms a circular opening at the bottom of the cylindrical cavity. The top surface of the cavity is an uncooled circular ceramic plate, also made of silicon carbide. This circular plate is supported by insulated standoffs to the outer casing. An annular plate made of Inconel 625 is attached to the bottom of the casing and supports the ceramic aperture cone.

Optical and Thermal Design

Analysis of concentration-type solar receivers requires that optical and thermal properties be considered. This is because the solar receiver is directly coupled to the optical system. The optical input to the receiver depends on the detailed characteristics of the receiver, the concentrator, and the orientation of these two major elements. Evaluation of the solar flux into the receiver is performed with a model in which the sun is treated as an extended, finite-size source. The resultant radiation transfer can be accurately analyzed by using cones, rather than optical rays, as the basic description for energy transport.

Incident solar flux distributions on the receiver cavity walls, as generated by the mathematical solar simulator, are presented in Figure 2 for the 85-kwt design point case. In equation form, the solar concentration ratio is defined as

$$CR_S \triangleq Q''/\rho \cdot S'' \cdot \eta_{coll} \qquad (1)$$

where Q'' is the heat flux impinging on the surface

ρ is the concentrator reflectivity

S'' is the local solar insolation

η_{coll} is the aperture/concentrator collector efficiency

Collector efficiency is defined as

$$\eta_{coll} \triangleq \frac{\text{energy collected in aperture opening}}{\text{energy reflected by concentrator}} \qquad (2)$$

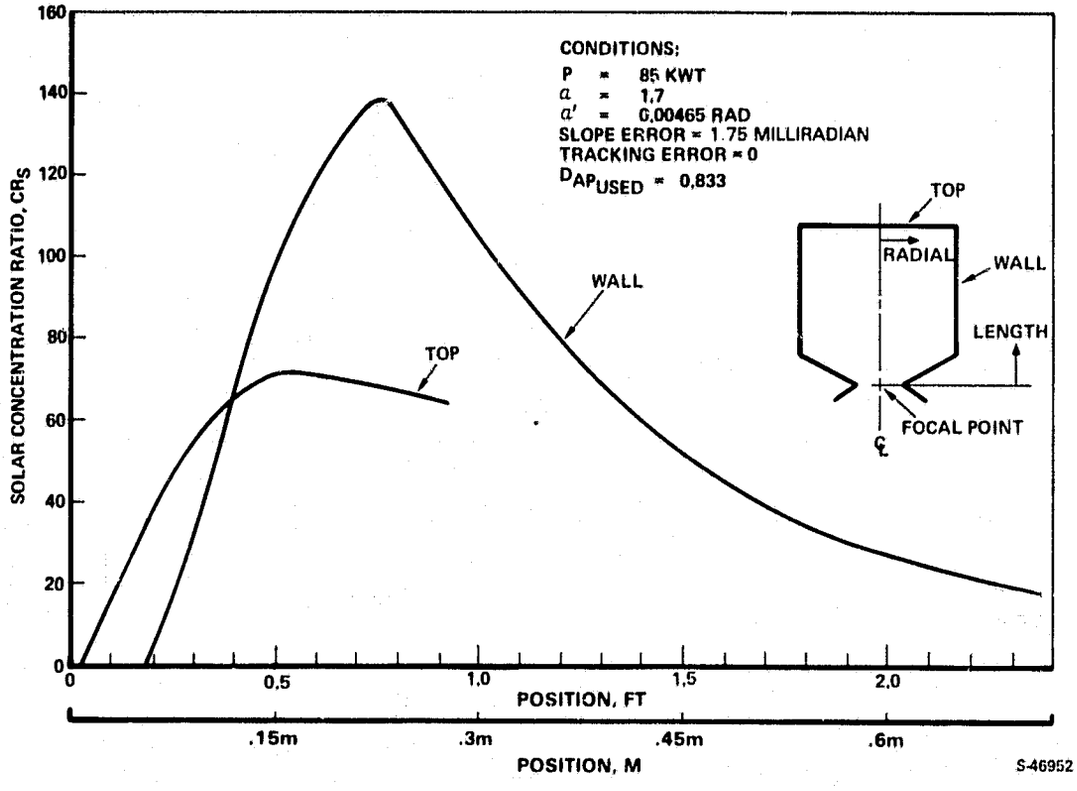

FIG. 2. CAVITY WALL SOLAR CONCENTRATION RATIO DISTRIBUTION

In Figure 2, the cylindrical cavity wall solar concentration ratio is shown as a function of cylinder length, as measured from the focal point. The solar concentration ratio for the closed end (top) is shown as a function of radial position, as measured from the receiver centerline. Conditions used in obtaining these plots also are indicated in Figure 2. This type of incident radiant flux information is a required input for a detailed thermal analysis of the solar receiver.

Thermal analysis of the receiver is performed by a finite-element thermal analyzer computer code developed by AiResearch. The cavity wall incident flux information is input to the computer code, along with fluid flow data and geometry specifications. Multiple reflections and reradiation characteristics inside the cavity are calculated by the following relationship:

$$\underline{B} - A^{-1}\underline{C} \tag{3}$$

where $\underline{B}$ is the radiosity column matrix

A is an N X N characteristic matrix

$\underline{C}$ is a temperature-dependent column matrix

Equation (3) assumes a gray body and diffuse emittance and reflections. For solar applications, the gray body assumption is acceptable for rough metal surfaces with high emissivities ($\sim$0.8). This is because the difference between the solar absorption and the metallic emissivity is relatively small for metallic surfaces with high emissivities.

The net heat flux lost from the i^{th} surface is obtained from the following equation:

$$Q''_i = \frac{1 - \varepsilon_i}{\varepsilon_i} (E_{b_i} - B_i) \tag{4}$$

where ε is the emissivity

E_b is the black body emissive power

Q" is the net heat flux lost from the i^{th} surface

The cavity wall temperature distribution resulting from a steady-state thermal analysis of the receiver design is shown in Figure 3 for the three cavity sections--the aperture conical end (nodes 5 and 6), the cylindrical wall (nodes 8 through 15), and the closed end (nodes 17 and 18). A direct physical connection between the cylindrical section at both the aperture end and the closed end has been avoided, thereby eliminating large localized thermal gradients between these sections. Because the fluid is single phase and the inlet and outlet temperatures are fixed, and because a relatively high fluid heat transfer conductance (hA) exists, the wall temperature profile is controlled by the fluid temperature. Thus, minor variations in the concentrator performance (e.g., slope error = 2 milliradians) will not significantly affect the cavity efficiency for the aperture size selected.

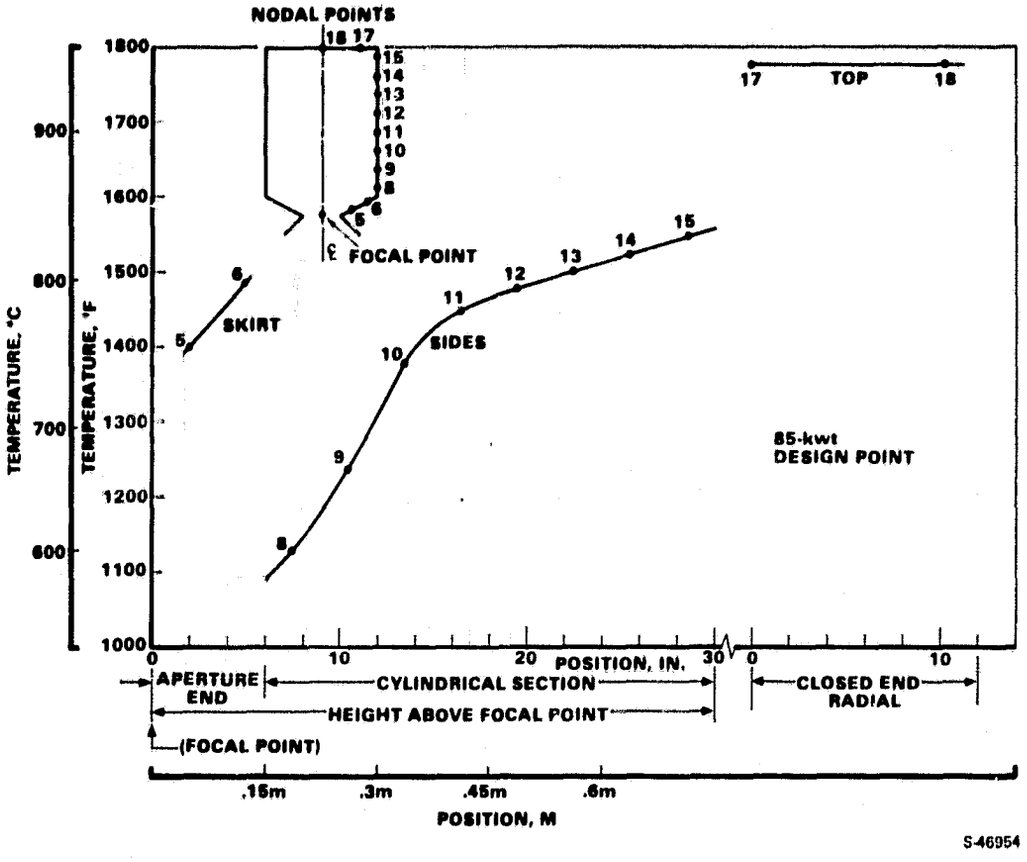

FIG. 3. STEADY-STATE CAVITY WALL TEMPERATURE DISTRIBUTION FOR 85-KWT DESIGN POINT CASE

Aperture convection losses are accounted for by scaling test data in the literature for open-cavity type solar receivers. This procedure indicates losses will amount to approximately 2 percent of the incident power for a 40.25-km/hr (25-mph) wind condition.

The steady-state thermal analysis includes a complete nodal temperature distribution throughout the receiver, fluid temperature rise, fluid pressure drop, cavity efficiency, and energy tabulation. Table 1 presents the energy bookkeeping summary and cavity efficiency calculation for the design point operating condition. The cavity efficiency presented is defined as

$$\eta_{cav} \triangleq \frac{\text{energy into fluid}}{\text{energy into aperture}} \tag{5}$$

Cavity efficiency as a function of thermal input energy for three different aperture sizes is shown in Figure 4. Note that the smallest aperture consistent with the concentrator optics is the most desirable.

TABLE 1

BRAYTON SOLAR RECEIVER PERFORMANCE

Thermal power level	85 kwt (nominal)
Design sun half-angle	0.007905 radian (slope error = 0.0573 deg, track error = 0 deg)
Actual sun half-angle	0.00465 radian
Incident solar flux	0.979 kw/m^2
Concentrator reflectivity	0.86
Energy bookkeeping	
Total energy into cavity, kwt (percent)	85.0 (100)
Energy to fluid, kwt (percent)	78.6 (92.5)
Energy losses, kwt (percent)	
Loss by radiation out aperture	3.62 (4.26)
Loss by convection out aperture*	1.70 (2.0)
Loss by radiation and convection from the outer surface ..	1.05 (1.24)
Cavity efficiency, percent	92.5

*Assumed 2-percent loss due to aperture convection losses.

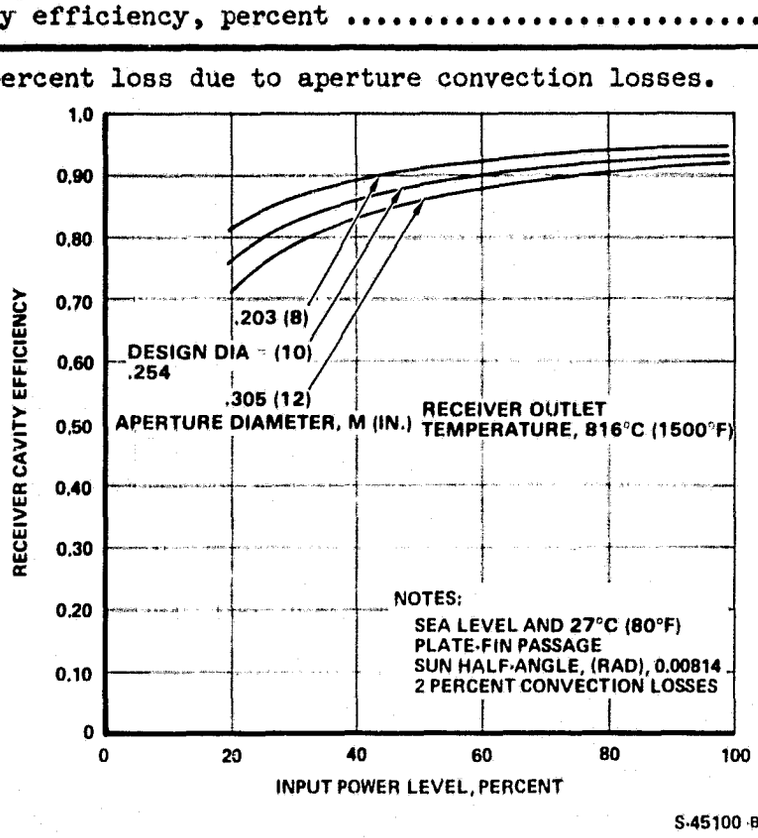

FIG. 4. BRAYTON SOLAR RECEIVER CAVITY EFFICIENCY AS A FUNCTION OF POWER LEVEL

Structural Design

The receiver heat exchanger is designed to withstand an operating pressure of 2.59 atm (38 psia) at a maximum temperature of 843°C (1550°F) and a proof pressure of 4.42 atm (65 psia) at room temperature without yielding. The fins brazed between the inner and outer walls of the heat exchanger react the internal pressure loads. The predicted life of the prototype heat exchanger unit is 6000 start/stop cycles or approximately 8 to 10 years.

The cavity panel heat exchanger is attached to the outer casing by four radial tubes located at two locations along its length. The upper set of support tubes allows for radial thermal growth and the bottom set allows for both radial and axial thermal growth. The aperture cone is supported from the case with insulated standoffs, as is the circular top plate.

Bellows on the air inlet and exit lines at the top of the receiver limit the loads that might be imposed on the heat exchanger from this source.

Test Program

As part of the development effort, one receiver heat exchanger with the appropriate ducting will be fabricated and assembled in the test device shown in Figure 5. A cylindrical electric heater is inserted in the test heat exchanger cavity. The heater consists of wire resistance elements arranged on the surface of the cylindrical heater. There are 10 separately controlled heating zones on the heater surface; this allows the imposition of the same net heat flux distribution on the heat exchanger wall that will be seen during operation with solar input. The assembly is installed in a low-pressure chamber that provides an argon cover gas for the electric heater assembly. Tests will be performed to obtain heat exchanger performance as well as to subject the heat exchanger to 500 startup and shutdown cycles.

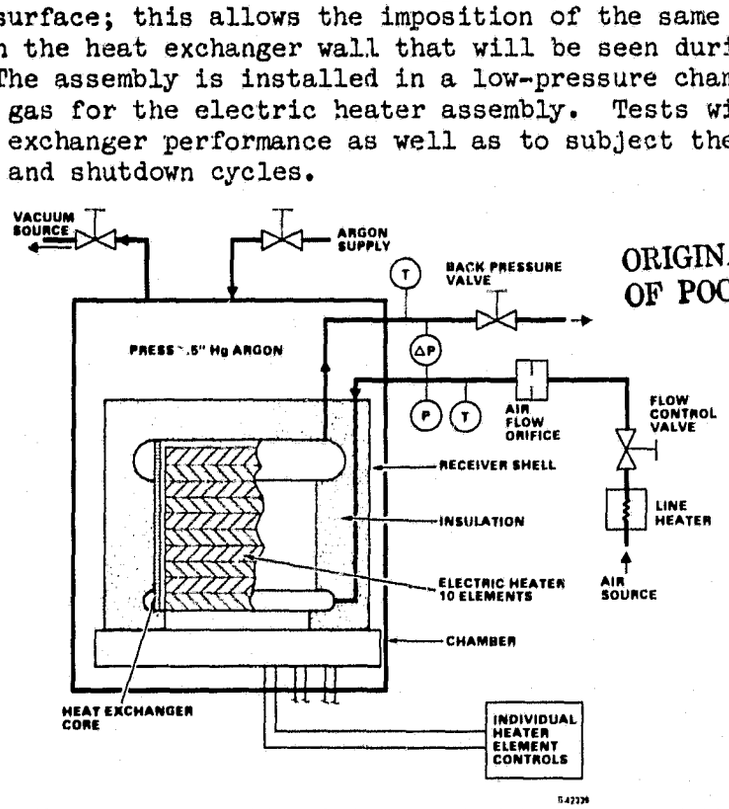

FIG. 5. HEAT EXCHANGER DEVELOPMENT TEST SETUP

STEAM RANKINE SOLAR RECEIVER

Design Requirements

The receiver is designed for two applications, each with a peak solar input of 85 kw. The first application is to supply heat to a steam power system and the second to supply process heat.

The steam power application is further divided so that in one case the receiver operates with a system employing reheat. In this case the boiler heats the inlet water at 17.22 MPa (2500 psi) and 49°C (300°F) to supply heat at 704°C (1300°F). The reheat section accepts steam at 1.20 MPa (175 pisa) and 343°C (650°F), heating it to 704°C (1300°F). The total pressure drop is not to exceed 10 percent $\Delta P/P$. Flow rate is determined from the energy balance.

The second steam power case eliminates the reheat section. The steam flow is routed directly from the discharge of the boiling section to the inlet of the reheat section. The flow rate is rebalanced to supply steam at 17.22 MPa (2500 psi) and 704°C (1300°F) at a $\Delta P/P$ of 10 percent.

The process steam application considered variable inlet temperatures and pressures without reheat up to the values defined for the steam power condition.

Receiver Description

The steam Rankine receiver is similar to the Brayton receiver in that they both use a 0.76-m (30-in.)-dia case and the same mounting provisions. Approximately 10.1 cm (4 in.) of insulation separates the case from the cavity heat transfer surfaces. The significant features of this receiver are shown in Figure 6. Two helical tube coils form the interior cavity walls. The preheat-boiling coil, located adjacent to the aperture, is a 1.11-cm (0.4375-in.) tube with a coil diameter of 0.43 m (17 in.) and a coil length of 0.371 m (14.6 in.). The reheat coil is a 1.8-cm (0.75-in.) tube with a coil diameter of 0.43 m (17 in.) and a length of 0.175 m (6.9 in.). Both coils are manufactured from Inconel 625 or type 347 stainless steel. These coils are brazed separately and mechanically joined together. The aperture assembly is the same as the Brayton receiver. The top of the receiver cavity is an uncooled ceramic plate, which is adjustable in the axial direction through the use of an adjustment screw located on the exterior case.

Thermal Design

The optical and thermal design procedures used for the Rankine receiver are similar to those of the Brayton receiver. However, a distinct difference affects this design as the fluid changes phase in the preheat-boiling section when single-phase heat transfer and basic flow friction data were used to predict the design heat transfer coefficients for liquid and steam. The correlations of Chen (1), below 70-percent quality, and Lockhart/Martinelli (2), two-phase flow above 70-percent quality, were used to establish coefficients of performance in the boiling region.

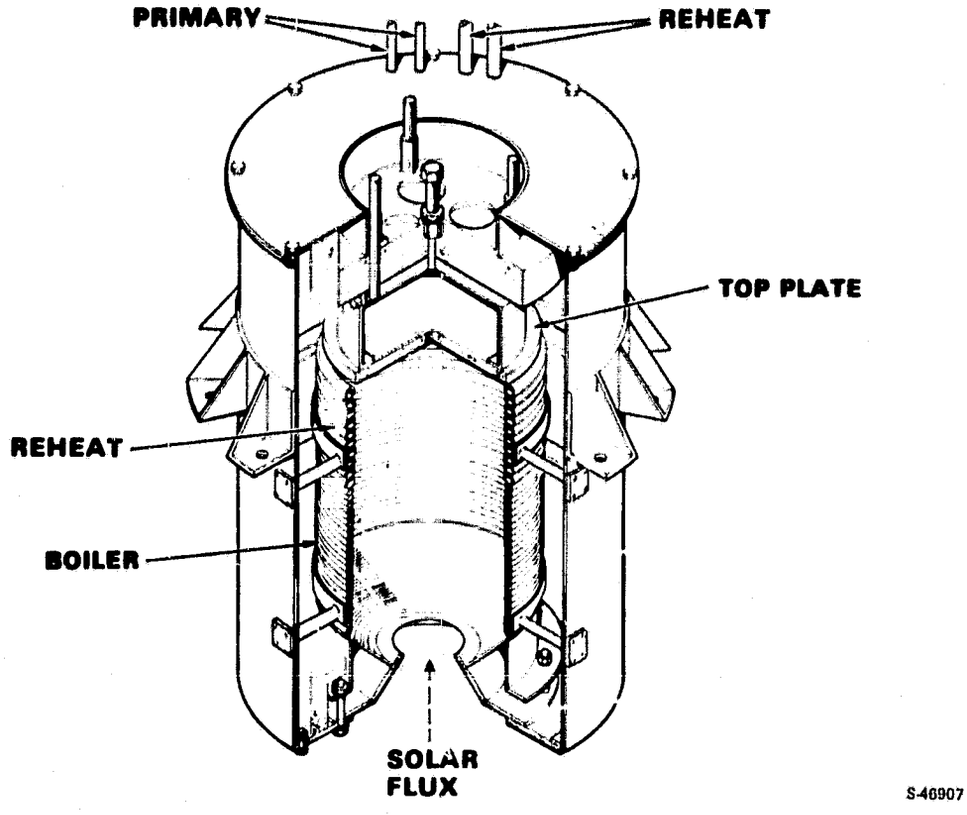

FIG. 6. PROTOTYPE STEAM RANKINE SOLAR RECEIVER

The cavity wall and fluid temperature distribution for a steady-state thermal analysis of the boiling and reheat application is shown in Figure 7. The steam outlet temperatures from the boiling and reheating sections are matched. The slope of the temperature curve at this location indicates that the match is highly dependent on flux distribution. Consequently, a sensitivity analysis was conducted. This was based on relocating the peak flux 7.62 cm (3 in.) toward the top end of the cavity and altering the distribution by reducing the peak flux 20 percent and distributing the energy toward the top of the cavity. The resulting temperature profile is shown in Figure 8. Since distribution variations of this magnitude were considered possible, a movable top end plate was included within the design. Repositioning the plate toward the aperture 4 cm (1.6 in.) rebalances the fluid temperature at 704°C (1300°F). This is accomplished by a combination of shielding of the reheat section and reradiation from the top plate to the remainder of the cavity. The energy bookkeeping summary and cavity efficiency for the boiling-reheat design requirement is shown in Table 2.

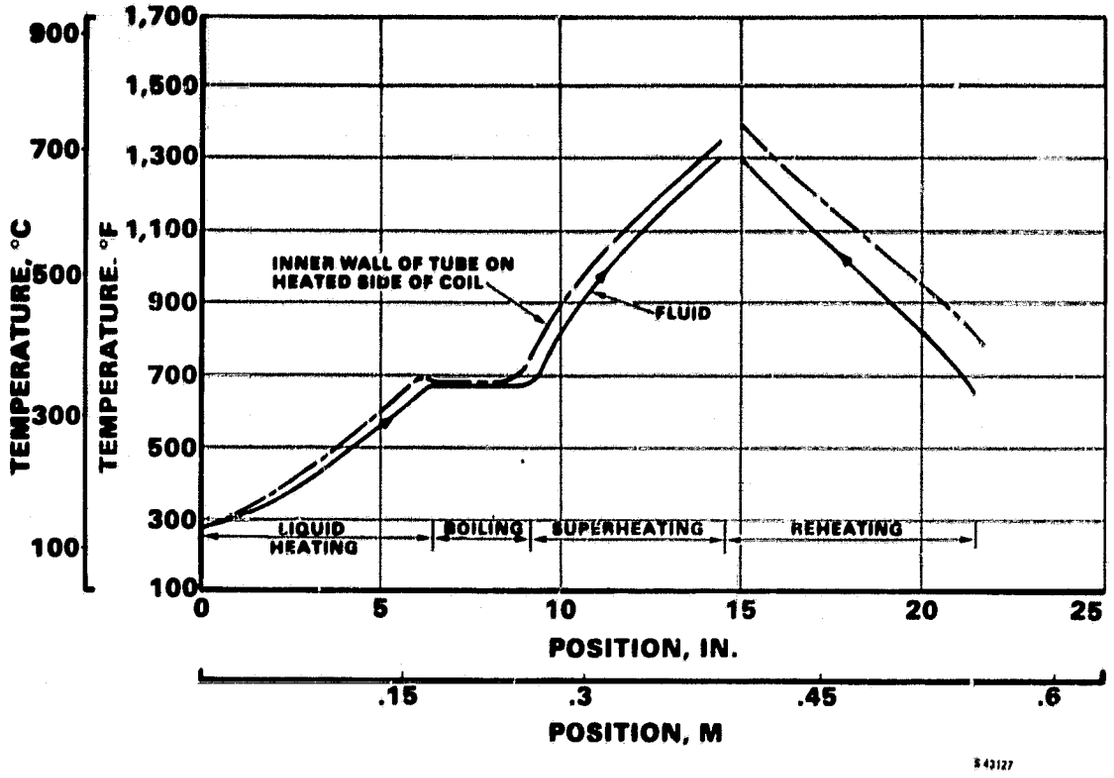

FIG. 7. AXIAL TEMPERATURE DISTRIBUTION WITH DESIGN FLUX

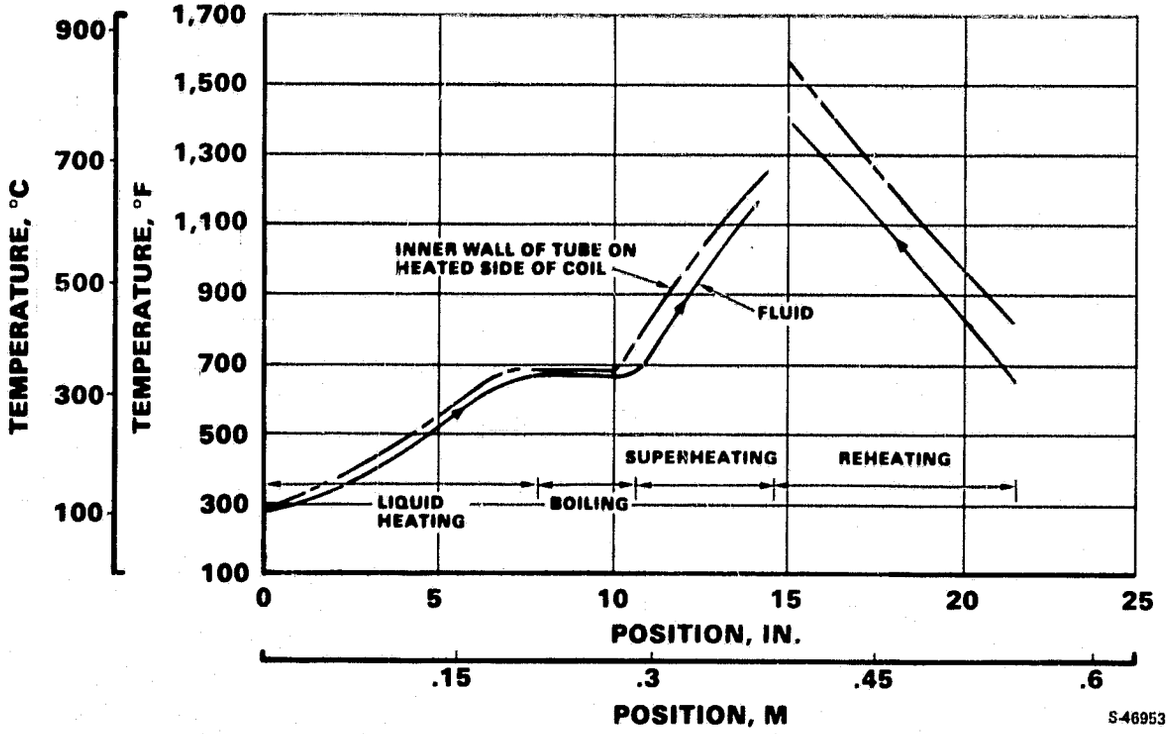

FIG. 8. AXIAL TEMPERATURE DISTRIBUTION WITH REDISTRIBUTED FLUX

TABLE 2

STEAM RANKINE SOLAR RECEIVER THERMAL PERFORMANCE SUMMARY

Solar input	85 kwth
Aperture radiation loss	1.3
Insulation loss	1.2
Assumed aperture assembly convection and radiation loss	2.5
Thermal power to fluid	80
Receiver efficiency	94 percent
Flow rate	71 kg/hr (157 lb/hr)
Pressure drop	
Boiler	2 percent
Reheat	10 percent
Without reheat	
Flow rate	89 kg/hr (196 lb/hr)
Pressure drop	3 percent

Structural Design

The receiver is designed to operate at a maximum pressure of 17.57 MPa (2550 psi) at 704°C (1300°F) and to withstand a proof pressure of 37.2 MPa (5400 psi) at room temperature.

By uncoupling the boiling and reheat coils the axial coil bending loads that would have occurred at this junction were avoided. The remaining stresses are the result of pressure and temperature differences acting on the tube cross section. A computer-aided stress analysis was used to determine the peak combined stresses occurring in a tube section operating at 371°C (700°F). The peak combined stress is 154 MPa (22.34 kpsi). Based on Inconel 625 mechanical properties, the projected life is greater than 1.10^5 cycles.

Test Program

A test program that is comparable to the one conducted on the Brayton receiver will be computed on a prototype unit. Operation at the design point will be verified and a cyclic thermal pressure test will be conducted.

ACKNOWLEDGEMENTS

I wish to thank Mr. M. Coombs, Mr. J. Eastwood, and the other members of the heat transfer and cryogenic engineering group of AiResearch Manufacturing Company for their assistance in preparing this paper.

REFERENCES

1. Chen, J., "A Correlation for Boiling Heat Transfer to Saturated Fluids in Convective Flow," ASME, 63 TTT 34, May 1, 1963.

2. Lockhart, R. W., and R. C. Martinelli, "Proposed Correlation of Data for Isothermal Two-Phase Two-Component Flow in Pipes," Chem. Eng. Progress, 45:39, 1974.